

CONSTRAINING THE AGE-ACTIVITY RELATION FOR COOL STARS: THE SDSS DR5 LOW-MASS STAR SPECTROSCOPIC SAMPLE

ANDREW A. WEST^{1,2}, SUZANNE L. HAWLEY³, JOHN J. BOCHANSKI³, KEVIN R. COVEY^{4,5}, I. NEILL REID⁶, SAURAV DHITAL⁷,
 ERIC J. HILTON³, MICHAEL MASUDA³

accepted for publication in AJ

ABSTRACT

We present a spectroscopic analysis of over 38,000 low-mass stars from the Sloan Digital Sky Survey (SDSS) Data Release 5 (DR5). Analysis of this unprecedentedly large sample confirms the previously detected decrease in the fraction of magnetically active stars (as traced by H α emission) as a function of vertical distance from the Galactic Plane. The magnitude and slope of this effect varies as a function of spectral type. Using simple 1-D dynamical models, we demonstrate that the drop in activity fraction can be explained by thin disk dynamical heating and a rapid decrease in magnetic activity. The timescale for this rapid activity decrease changes according to the spectral type. By comparing our data to the simulations, we calibrate the age-activity relation at each M dwarf spectral type. We also present evidence for a possible decrease in the metallicity as a function of height above the Galactic Plane. In addition to our activity analysis, we provide line measurements, molecular band indices, colors, radial velocities, 3-D space motions and mean properties as a function of spectral type for the SDSS DR5 low-mass star sample.

Subject headings: solar neighborhood — stars: low-mass, brown dwarfs — stars: activity — stars: late-type — Galaxy: structure — Galaxy: kinematics and dynamics

1. INTRODUCTION

As the most numerous stellar constituents of the Milky Way, M dwarfs are an ideal population for tracing the structure and evolution of the stellar thin disk. A number of studies have utilized the ubiquity of M dwarfs to study the dynamics and distribution of stars in the Solar neighborhood (Wielen 1977; Weis & Uppgren 1995; Reid et al. 1995; Hawley et al. 1996; Bochanski et al. 2007b). Many M dwarfs also host intense magnetic dynamos that give rise to chromospheric and coronal heating, producing emission from the x-ray to the radio. Over 30 years ago Wilson and Woolley (1970) found a link between magnetic activity (as traced by the CaII emission strength) and the orbits of more than 300 nearby late-type dwarfs. Their study concluded that magnetic activity in these stars was directly related to their age. Subsequent studies over the following decades have found a similar connection between age and activity in low-mass stars (Wielen 1977; Giampapa & Liebert 1986; Soderblom, Duncan & Johnson 1991; Hawley et al. 1996; Hawley, Tourtellot & Reid 1999; Hawley, Reid & Tourtellot 2000).

The mechanism that controls magnetic activity in M dwarfs is still unknown. In the Sun, magnetic field generation has a strong connection to the Sun's rotation. Helioseismology has indicated that the boundary between the convective and the radiative zones (known as

the tachocline) creates a rotational shear; the convective zone undergoes differential rotation, while the radiative zone rotates like a solid body (Parker 1993; Ossendrijver 2003; Thompson et al. 2003). The tachocline allows magnetic fields to be generated, stored and ultimately rise to the surface where they emerge as magnetic loops. These loops drive the heating of the stellar chromosphere and corona, resulting in dramatic stellar flares and lower level quiescent magnetic activity. Rotation in solar type stars slows with time and as a result, activity decreases. Skumanich (1972) found that both activity (as measured by Ca II emission) and rotation decrease over time as a power law $t^{-0.5}$. Subsequent studies confirmed the Skumanich age/rotation-activity relation but found that the slope of the power law may change as a function of spectral type and that non-power law functions are not ruled out (Barry 1988; Soderblom et al. 1991). However, after a spectral type of \sim M3 (0.35 M_{\odot} ; Reid & Hawley 2005; Chabrier & Baraffe 1997), stars become fully convective and the tachocline presumably disappears. This transition marks an important change in the stellar interior that must affect the production and storage of internal magnetic fields.

Many studies have found evidence that the age-activity relation extends into the M dwarf regime. Eggen (1990) observed a Skumanich type power law decay in activity strength as a function of age. Larger samples of M dwarfs have added further evidence to the hypothesis that the magnetic activity in M dwarfs slowly decreases over time (Fleming, Schmitt & Giampapa 1995; Gizis, Reid & Hawley 2002). There are also data that support the hypothesis that activity in M dwarfs may have a finite lifetime. Stauffer et al. (1994) suggested that activity may not be present in the more massive M dwarfs in the Pleiades. Hawley et al. (2000) confirmed the Stauffer et al. (1994) claim by observing a sample of clusters

¹ Corresponding author: awest@astro.berkeley.edu

² Astronomy Department, University of California, 601 Campbell Hall, Berkeley, CA 94720-3411

³ Department of Astronomy, University of Washington, Box 351580, Seattle, WA 98195

⁴ Harvard-Smithsonian Center for Astrophysics, 60 Garden Street, Cambridge MA 02138

⁵ Spitzer Fellow

⁶ Space Telescope Science Institute, 3700 San Martin Drive, Baltimore, MD 21218

⁷ Department of Physics & Astronomy, Vanderbilt University, Nashville, TN 37235

that spanned several Gyrs in age. They were able to calibrate the activity lifetimes for early type M dwarfs by observing the color at which activity (as traced by spectroscopically observed $H\alpha$ emission) was no longer present. Because of the small sample size, the derived age-activity relation serves as a lower limit at a given color or spectral type. Silvestri et al. (2006) also argued for finite activity lifetimes by observing M dwarfs in binary systems with white dwarfs, finding no activity in the companions of the coolest, and therefore oldest white dwarfs. However, accurate activity lifetimes could not be calculated for the M dwarfs due to uncertainties in the pre-white dwarf ages, binary effects and small sample sizes. A larger spectroscopic sample is required to further constrain the activity-age relation in both nearby clusters and the field.

The advent of large surveys such as the Sloan Digital Sky Survey (SDSS; York et al. 2000) and the Two Micron All Sky Survey (2MASS; Cutri et al. 2003) has created optical and infrared catalogs of several million M dwarfs. In addition to the photometric data, the SDSS has obtained spectra for over 50,000 M dwarfs and the numbers continue to increase as SDSS-II (Adelman-McCarthy et al. 2007b) pushes to lower Galactic latitudes. Recently these surveys have been utilized to examine the statistical properties of M dwarfs in a variety of capacities, including analyses of mean M dwarf colors and spectroscopic properties (Hawley et al. 2002; West et al. 2004; hereafter W04; West, Walkowicz & Hawley 2005; Bochanski et al. 2007a; Covey et al. 2007), computing the dynamics of the Milky Way (West et al. 2006; hereafter W06; Bochanski et al. 2007b) and the detailed investigation of chromospheric magnetic activity (W04; W06; Silvestri et al. 2006; Bochanski et al. 2007a). The activity studies of W04 and W06 used SDSS spectra to show that the fraction of active M7 stars decreases with vertical distance from the Galactic Plane, further evidence of an age-activity relation. By comparing the data to simple dynamical simulations, W06 argued that the observed trend results from the combination of a rapid decrease in magnetic activity after 6-7 Gyrs and the correlation between age and height above the Galactic Plane introduced by dynamical heating of the M7 stars. A larger sample of low-mass star spectra allows for the obvious extension of the W06 study to all M dwarf spectral types. From this new statistical platform it is now possible to derive an age-activity relation for the entire M dwarf sequence and to investigate how this relation changes across the M3-M4 convective boundary.

In this paper we present a catalog of more than 44,000 spectroscopically confirmed M dwarfs from the SDSS. We describe the data, which are publically available, in §2. We present the mean sample characteristics and an analysis of the magnetic activity in §3. In §4, we compare our data to a series of dynamical simulations and derive an age-activity relation for low-mass dwarfs. We summarize these results in §5.

2. DATA

The SDSS (Gunn et al. 1998; Fukugita et al. 1996; York et al. 2000; Hogg et al. 2001; Gunn et al. 2006; Ivezić et al. 2004; Pier et al. 2003; Smith et al. 2002; Stoughton et al. 2002; Tucker et al. 2006) provides excellent quality spectroscopic and photometric data for

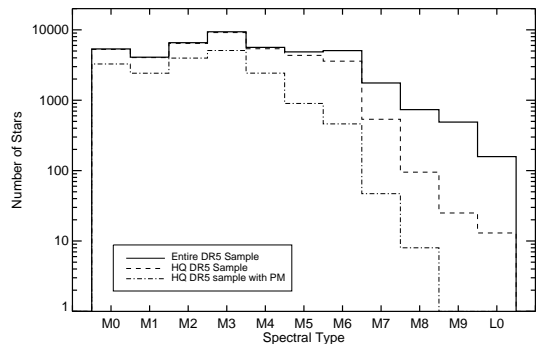


FIG. 1.— Spectral type distribution of the SDSS DR5 low-mass star spectroscopic sample. The total sample (solid) contains over 44,000 spectroscopically confirmed M and L-type dwarfs. Our analysis is confined to a high quality subsample (dashed) and a high quality subsample with measured proper motions (dot-dashed) which have over 38,000 and 20,000 stars respectively. See text for more details.

examining the properties of low-mass dwarfs. Our sample was drawn from the SDSS Data Release 5 (DR5; Adelman-McCarthy 2007a) and includes spectra from several of the “special plates” that are not part of the standard SDSS survey⁸. A total of 49933 stars were selected from the SDSS spectroscopic database based on the colors typical of M dwarfs ($r - i > 0.53$ and $i - z > 0.3$; West et al. 2005) and a standard set of SDSS processing flags (SATURATED, BRIGHT, NODEBLEND, INTERP_CENTER, BAD_COUNTS_ERROR, PEAK_CENTER, NOTCHECKED, and NOPROFILE were all required to be unset).⁹ Each spectrum was processed using the HAMMER stellar spectral-typing facility (Covey et al. 2007). The HAMMER determines the spectral type of each star using measurements of molecular bands and line strengths. We examined a subset of the spectra by eye and confirmed that the spectral types given by the HAMMER were accurate to within 1 subtype. We also limited our study to spectral types M0-L0. The HAMMER was able to successfully spectral type 44084 of the stars. Most of the spectra that were not typed were either low signal-to-noise or bad spectra. The spectral type distribution of the DR5 low-mass star spectroscopic sample is shown in Figure 1.

To ensure a statistically robust sample, we removed stars with 1) line-of-sight r -band extinction > 0.5 ; 2) colors consistent with having a white dwarf companion (Smolčić et al. 2004); and 3) measured radial velocities $> 500 \text{ km s}^{-1}$ (spurious velocities). The resulting high quality dataset contains 38835 stars, roughly 4 times the number of stars used in the W04 study.

The magnetic activity of each star was assigned based on its measured $H\alpha$ emission line strength. Although other emission lines can be used as activity indicators (e.g. CaII H \& K), our study defines an active star as one that has $H\alpha$ emission in its spectrum. $H\alpha$ EWs were measured by the HAMMER, which now includes most of the magnetic activity analysis described in W04. We assessed the accuracy of our activity analysis by running Monte Carlo simulations to test how well we could mea-

⁸ see <http://www.sdss.org/dr5/products/spectra/special.html>

⁹ See <http://www.sdss.org/dr5/products/catalogs/flags.html> for more information on SDSS flags

sure the $H\alpha$ emission line at a specific spectral type and for a given signal-to-noise spectrum. Using the Bochanski inactive templates (Bochanski et al. 2007a), we added noise and an emission line to each spectral type and then used our software to measure the $H\alpha$ EW 1000 times for each variation of noise, spectral type and emission strength. We found that at a signal-to-noise ratio (measured near $H\alpha$) of 3 and an $H\alpha$ EW of 1\AA (the same parameters used in previous studies; e.g. W04, W06), we could accurately recover the $H\alpha$ emission over 96% of the time for all spectral types. This agrees with the less than 4% error in assigning activity status that was estimated in W04.

After running the stars through the HAMMER, we used the method of Walkowicz, Hawley & West (2004) to compute the ratio of luminosity in the $H\alpha$ line to the bolometric luminosity ($L_{H\alpha}/L_{bol}$) for all stars in the sample. We adopted the color derived ($i - z$) χ values for this calculation. Distances to all stars were calculated using the photometric parallax methods of West et al. (2005) and Davenport et al. (2006). Using the positions and distances of each star, Galactic height was computed assuming the Sun is 15 pc above the Plane (Cohen 1995; Ng et al. 1997; Binney et al. 1997).

We used the SDSS/USNO-B matched catalog (Munn et al. 2004) to obtain proper motions. The SDSS/USNO-B catalog uses SDSS galaxies to recalibrate the USNO-B positions as well as includes SDSS stellar astrometry as an additional epoch for improved proper motion measurements. The USNO-B proper motions were obtained for 27285 of the SDSS stars (many stars were not matched due to the relative shallowness of the USNO-B catalog). Applying the same quality cuts as above, we arrived at a proper motion sample of 20160 stars. Radial velocities were measured for all SDSS stars using the method described in Bochanski et al. (2007a), employing co-added, zero-velocity SDSS spectra which were used to create high signal-to-noise ratio radial velocity templates. Our derived radial velocities are accurate to within $\sim 5 \text{ km s}^{-1}$ (Bochanski et al. 2007a). Using these proper motions the derived distances and the radial velocities, space motions were computed for all SDSS stars with measured proper motions.

We also matched our spectroscopic sample to the 2MASS point source catalog and found matches for 37845 of our stars. Although the infrared colors are not a vital part of our analysis, we include them in order to compute statistically robust 2MASS colors as a function of spectral type and will include them in the online electronic tables (see below).

The measured quantities for the SDSS DR5 low-mass star spectroscopic sample are available for electronic download for use by the astronomical community¹⁰. The individual spectra are available at the SDSS catalog archive server¹¹. It is important to note that these data do not represent a complete sample and that spectral targeting introduces a variety of selection effects. However, the sample covers a large range of values for many of the physical attributes of the stars, including activity, metallicity and Galactic motion, making an accurate

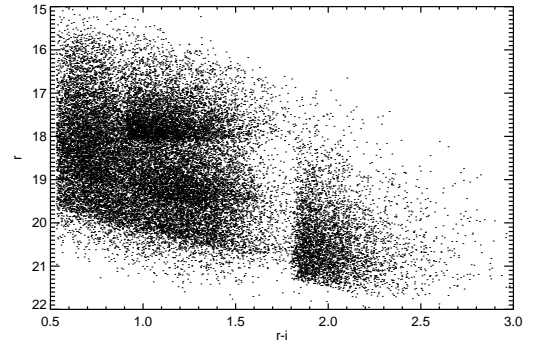


FIG. 2.— The color-apparent magnitude distribution for the sample. The blue “edge” is our color selection described above. The range of magnitudes is constrained by both the bright and faint limits of SDSS spectroscopy (Stoughton et al. 2002; Strauss et al. 2002) as well as our requirement that none of the stars be saturated in the photometric data. The gaps and overdense regions in color-magnitude space do not represent the actual distribution of stars but are a reflection of the SDSS spectroscopic targeting selection criteria, which are not designed to sample stars in a complete, or even uniform, manner.

activity analysis with this sample possible. In addition, because most of the derived quantities are computed by automatic routines, values for a small percentage of individual stars will be incorrect. Large statistical results should not be affected by these small errors. Users are nevertheless cautioned to understand the origins of the data before using them indiscriminately.

3. OBSERVATIONAL RESULTS

Table 1 gives the median and rms scatter (in parentheses) of the SDSS and 2MASS colors at each spectral type. The stars used to compute these values were selected to have small measurement errors and thus, the scatter represents the intrinsic scatter of the stellar locus and not the uncertainties in the median measurement. SDSS spectroscopic targeting does not uniformly sample the stellar locus, possibly introducing a bias to our derived colors. The $u - g$ and $g - r$ colors were not shown because of the large influence that metallicity has on the $g - r$ colors (West et al. 2004; Bochanski et al. 2007a) and the large uncertainties in the u -band fluxes for most of the sample stars. The SDSS colors are in excellent agreement with the previous results found in West et al. (2005) and Bochanski et al. (2007a). Because of the larger sample size, our 2MASS colors supersede those reported in Hawley et al. (2002), West et al. (2005) and Covey et al. (2007). Figure 2 shows the color-apparent magnitude distribution for the sample. The blue “edge” is our color selection described above. The range of magnitudes is constrained by both the bright and faint limits of SDSS spectroscopy (Stoughton et al. 2002; Strauss et al. 2002) as well as our requirement that none of the stars be saturated in the photometric data. The gaps and overdense regions in color-magnitude space do not represent the actual distribution of stars but are a reflection of the SDSS spectroscopic targeting selection criteria, which are not designed to sample stars in a complete, or even uniform, manner. Figure 2 also helps to demonstrate why some of the computed colors from Table 1 may be affected by selection biases. Clearly, an analysis of the luminosity function of low mass stars cannot be carried out with these data, but is currently being ad-

¹⁰ Measured quantities can be obtained electronically using the CDS VizieR database <http://vizier.u-strasbg.fr/viz-bin/VizieR>

¹¹ <http://cas.sdss.org/astrodr5/en>

TABLE 1
COLORS OF LATE-TYPE DWARFS

Spectral Type	N _{SDSS} ^a	N _{2MASS} ^a	$r - i$	$i - z$	$z - J$	$J - H$	$H - K$
M0	4945	1962	0.66 (0.12)	0.38 (0.07)	1.23 (0.19)	0.65 (0.10)	0.18 (0.14)
M1	3721	1504	0.82 (0.18)	0.46 (0.07)	1.27 (0.21)	0.64 (0.10)	0.21 (0.13)
M2	6105	2472	1.00 (0.13)	0.55 (0.08)	1.31 (0.17)	0.62 (0.10)	0.22 (0.12)
M3	8609	3752	1.21 (0.16)	0.65 (0.08)	1.37 (0.17)	0.60 (0.10)	0.24 (0.14)
M4	4984	2126	1.46 (0.15)	0.79 (0.09)	1.45 (0.16)	0.59 (0.10)	0.27 (0.13)
M5	3608	879	1.91 (0.13)	1.06 (0.07)	1.61 (0.11)	0.59 (0.11)	0.31 (0.14)
M6	2674	570	2.11 (0.14)	1.16 (0.07)	1.71 (0.10)	0.60 (0.11)	0.33 (0.14)
M7	382	306	2.50 (0.18)	1.37 (0.09)	1.85 (0.10)	0.62 (0.09)	0.36 (0.11)
M8	74	147	2.73 (0.25)	1.58 (0.15)	2.04 (0.12)	0.66 (0.06)	0.40 (0.06)
M9	13	69	2.81 (0.21)	1.76 (0.08)	2.25 (0.09)	0.70 (0.08)	0.42 (0.06)
L0	10	31	2.49 (0.09)	1.84 (0.06)	2.45 (0.11)	0.77 (0.06)	0.50 (0.04)

NOTE. — The median and rms scatter (in parentheses) of the SDSS-2MASS colors at each spectral type. Because the stars used to compute these values have small measurement errors, the scatter represents the intrinsic scatter of the stellar locus and not the uncertainties in the median measurement. SDSS spectroscopic targeting does not uniformly sample the stellar locus, possibly introducing a bias to our derived colors. The $u - g$ and $g - r$ colors are not shown because of the large influence that metallicity has on the $g - r$ colors (West et al. 2004; Bochanski et al. 2007a) and the large uncertainties in the u -band fluxes for most of the sample stars.

^a Only stars with magnitude uncertainties smaller than 0.05 were used to compute the median colors

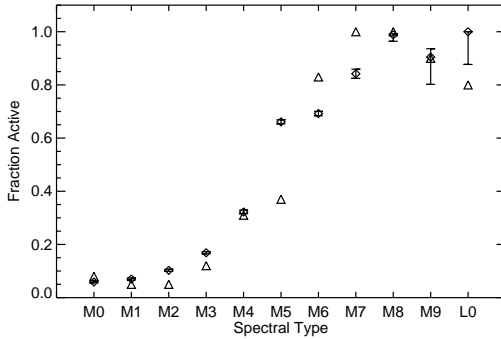


FIG. 3.— Fraction of active stars as a function of spectral type for the DR5 spectroscopic sample (diamonds). At earlier types ($< M7$) this distribution resembles that of previous studies (triangles; Hawley et al. 1996; Gizis et al. 2000; W04). However, we do not see a turnover in the activity fraction in the latest types as seen previously. This is likely a result of our strict quality cuts, which remove the distant, late-type stars from the sample. The more distant stars are more likely to be older and therefore inactive. However, the low signal-to-noise in those spectra does not allow us to be certain of their activity state and they are therefore excluded from the analysis.

dressed using the SDSS photometric data (Covey et al. 2008; Bochanski et al. 2008).

3.1. Activity

Applying the aforementioned signal-to-noise and EW cuts (3 and 1 Å respectively) to our activity analysis yields an updated distribution of activity fraction as a function of spectral type (Figure 3). At earlier types ($< M7$) this distribution resembles that of previous studies (Hawley et al. 1996; Gizis et al. 2000; W04). However, the later types do not show the same decrease in activity fraction seen previously (W04; Schmidt et al. 2007). This is likely a result of our strict quality cuts, which removes the distant, late-type stars from the sample. The more distant stars are more likely to be older and therefore inactive. However, the low signal-to-noise in those spectra makes their activity state uncertain, and they are therefore excluded from the analysis.

Figure 3 highlights an important point about the selection effects surrounding previous determinations of the

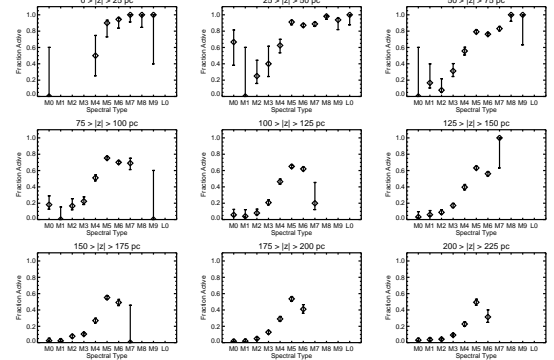


FIG. 4.— The fraction of active stars as a function of spectral type for 9 different regions in vertical distance from the Plane. By tracing individual spectral types over each distance bin, we see that distance plays an important role in determining the shape of Figure 3; most of the stars are active in the nearby bins and the activity fraction declines as we examine more distant stars.

activity fraction as a function of spectral type. Because the activity fraction at a given spectral type changes as a function of Galactic height (W04; W06), the sample selection will bias the observed activity fraction. We demonstrate this effect by plotting the activity fraction as a function of spectral type and constraining the absolute Galactic height of the stars to 9 different regions (Figure 4). It is clear that the volume in which the data are observed plays a large role in the resulting activity fractions.

The distance effect can be clearly seen by expanding on the study of W06 and examining how the activity fraction changes as a function of vertical height for each spectral type. Figure 5 shows the activity fraction as a function of absolute height above the Plane for spectral types M0-M8 (data have been folded across the Plane to increase the signal). There are not enough stars in the later-type bins to justify their analysis. In almost every case, the stars closer to the Galactic Plane have larger activity fractions than those further from the Plane. The amplitudes and slopes of the decrease are different for each spectral type. Dynamical models with activity lifetimes are fit to these data and discussed in §4.

As previously seen in M7 dwarfs (W06), most of the

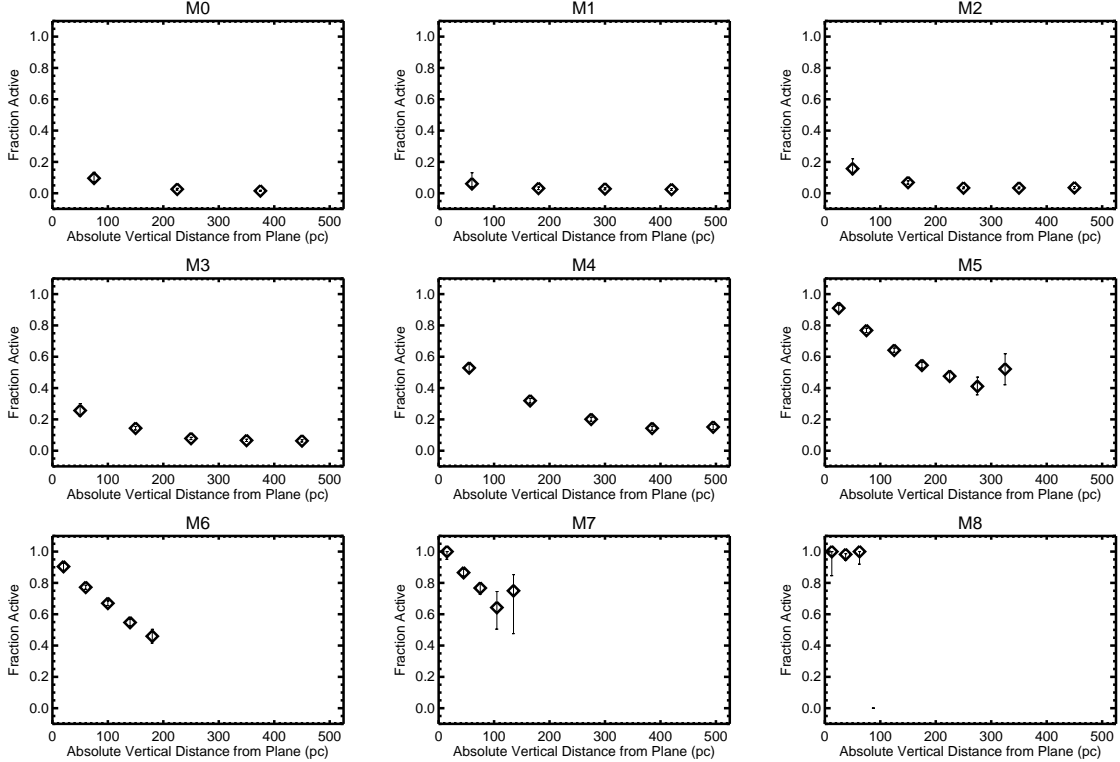


FIG. 5.— The fraction of active stars as a function of absolute distance from the Galactic Plane for M0-M8 dwarfs. The activity fraction decreases with Galactic height at all spectral types. The magnitude and slope of the decline varies as a function of spectral type. This effect is likely caused by the combination of thin disk dynamical heating and a rapid decrease of magnetic activity after a characteristic time.

spectral types show some evidence that the level of activity (quantified by $L_{H\alpha}/L_{bol}$; Hawley et al. 1996) also decreases as a function of vertical height above the Plane. Figure 6 shows the mean $L_{H\alpha}/L_{bol}$ distribution for M2-M7 stars as a function of vertical distance from the Plane. The other types were excluded because of the small number of active stars at early spectral types and small vertical extent at late spectral types. Although the spread of the distribution is large (large error bars) in each bin, the uncertainty in the mean (small error bars) is small, and indicates a small but significant decrease in activity with distance. This trend runs opposite to what one might expect from a magnitude-limited selection effect; stars with more activity should be easier to see further away. This decrease is marginally consistent with a Skumanich (1972) type power law age-activity relation ($t^{-\alpha}$). However, a unique value of α cannot explain all of the trends, and the activity decrease is likely more complicated.

In addition, the lack of stars with small $L_{H\alpha}/L_{bol}$ at small distances from the Plane suggests that activity does not continue a slow decline forever, but undergoes a rapid decrease at some point during a star's lifetime. There are stars in the DR5 sample that have $H\alpha$ EW $< 1\text{\AA}$ but do not get included in our main study and have smaller $L_{H\alpha}/L_{bol}$ values. However, there is still a population of nearby, high signal-to-noise stars in which we could detect $H\alpha$ activity if it were there - but we don't. Our ability to observe inactive stars is confirmed by other studies including the high resolution spectroscopic study of Rauscher & Marcy (2006) and the Bochanski et al. (2007a) spectral templates, where thousands of our inactive SDSS spectra were co-added to produce extremely

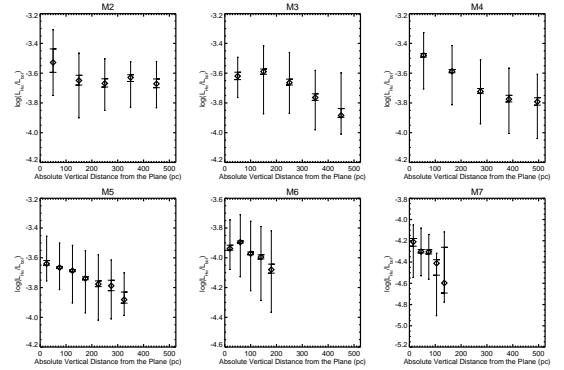


FIG. 6.— Median $L_{H\alpha}/L_{bol}$ as a function of absolute vertical distance from the Plane. The narrow error bars indicate the spread of $L_{H\alpha}/L_{bol}$ values while the wide error bars are the uncertainties in the median relations. Although the spread in $L_{H\alpha}/L_{bol}$ is large at each bin, there is a slight but significant decreasing trend with distance from the Galactic Plane. The decrease is marginally consistent with a Skumanich (1972) type power law age-activity relation ($t^{-\alpha}$). However, a unique value of α cannot explain all of the trends and the activity decrease is likely more complicated.

high signal-to-noise template spectra. The inactive templates as well as many of the Rauscher & Marcy (2006) stars show no signs of $H\alpha$ activity, confirming our ability to measure a star when it is in the inactive phase.

3.2. Metallicity

In addition to having less activity and greater dynamical heating, stars formed earlier in the Galaxy's history should have fewer metals; we should see a decrease in metallicity as a function of vertical distance from the Plane. Currently, there are no robust techniques for

translating low resolution spectra of M dwarfs to an absolute metallicity scale. Woolf and Wallerstein (2006) attempted to calibrate M dwarf metallicities using the molecular indices described in previous studies (Reid, Hawley & Gizis 1995; Gizis 1997), but were thwarted by small sample size. High resolution follow-up of recent large surveys of cool, nearby stars that span a range of metallicities (e.g. this sample; Marshall 2007), will allow for larger datasets to properly calibrate the metallicity scale. In the meantime, we can use molecular indices to determine relative metal content. Recent studies have used a combination of the Gizis (1997) indices (CaH2, CaH3 and TiO5) to identify low mass subdwarfs and extreme subdwarfs (Lepine, Shara & Rich 2003; Burgasser & Kirkpatrick 2006). We adapt the Lepine two-dimensional metallicity space to a single ratio, $(\text{CaH2}+\text{CaH3})/\text{TiO5}$, and use this as a proxy for metallicity at a given spectral type (a similar technique was used in Bochanski et al. 2007b).

Figure 7 shows the metal sensitive ratio $((\text{CaH2}+\text{CaH3})/\text{TiO5})$ as a function of vertical distance above the Plane for M0-M8 dwarfs. A decrease in metallicity as a function of Galactic height is clearly evident, indicating that the more distant stars have fewer metals. For the latest-type dwarfs, the small number of usable stars does not allow for an accurate analysis, but for the early-mid types the metallicity trend is both pronounced and significant. In the future, when molecular indices can be reliably tied to an absolute metallicity scale, we will be able to use each spectral type independently to calibrate the metallicity evolution of the Milky Way disk.

4. SIMULATIONS

We used the simple 1-D dynamical model described in W06 to trace the vertical dynamics of stars as a function of time. For each spectral type, we assumed a constant star formation rate, and injected a new population of 50 stars at the Galactic midplane every 200 Myr, for a total simulation time of 10 Gyrs. Each new group of stars began with a randomly drawn velocity dispersion of 8 km s^{-1} (Binney et al. 2000) and had a new position and velocity computed every 0.1 Myr. We used the “leap-frog” integration technique (Press et al. 1992) and the vertical Galactic potential from Kuijken & Gilmore (1989) and Siebert et al. (2003) to track the vertical dynamics of each star in the simulation.

We simulated dynamical heating by altering the velocities (energies) of stars such that their new velocity dispersions would match a $\sigma \propto t^{0.5}$ relation (Wielen 1977; Fuchs et al. 2001; Häneninen & Flynn 2002). The velocities were also scaled by the square-root of the mass appropriate for each type (as defined by Reid & Hawley 2005). We varied the heating energy about this mean value and added randomly drawn velocities when stars were within a given distance from the Plane. This distance (or “region of influence”; see W06) is a way to parameterize the cross section of interactions with molecular clouds during a vertical Plane crossing and it is modeled to be symmetric about the Galactic midplane. In a given orbit, a star may have no interactions with molecular clouds, or it may run into the full extent of a molecular region. Thus, to first order, “the regions of influence” can be thought of as the product of the scale height of molec-

ular gas and the fraction of Plane crossings that result in a dynamical kick. The size of the “region of influence” is varied from $\pm 0.5 \text{ pc}$ to $\pm 5 \text{ pc}$ in intervals of 0.5 pc . In total we ran 70 simulations for each M dwarf spectral type. Our simulations tracked the velocity, position and age of each star.

After the dynamical simulations were complete, we introduced a timescale for magnetic activity to the simulated data. Specifically, we assigned an activity lifetime to every star of a given spectral type. We varied these lifetimes from 0 Gyr to 9 Gyr in 0.1 Gyr intervals for each individual simulation. From the resulting data, we can derive activity fractions as a function of vertical distance from the Plane and examine how the simulated properties compare to the observed data.

We compared the simulated activity fractions to the observed activity fraction as a function of galactic height and performed a chi-squared minimization, fitting for “region of influence” size, dynamical heating energy and activity lifetime. Because the “region of influence” should be the same for all spectral types, we first solved for the best-fit value and found it to be 1 pc, slightly smaller than the 3 pc found in W06. Although 1 pc is close to the edge of the explored grid (0.5 pc), it produces a significantly better fit to the data as compared to the runs that use 0.5 or 1.5 pc values. Then, using a fixed “region of influence” of 1 pc, the energies and activity lifetimes were determined for each spectral type. Figure 8 shows the observed activity fraction as a function of vertical distance from the Plane with the simulated trends overplotted for the best-fit simulations.

To ensure that our simulations were producing dynamically accurate results, we compared the vertical velocity dispersions from our proper motion matched sample to the simulated velocity dispersions. The velocity dispersions were measured using the probability analysis described in Bochanski et al. 2007b (see also Reid et al. 1995). Figure 9 shows the velocity dispersions as a function of absolute vertical distance from the Plane for both the DR5 sample and the simulations. For several spectral types, there are a limited number of stars with good proper motions. Therefore, only the M1-M6 spectral types have been included. The data and model velocities are in excellent agreement for most of the measured velocity bins. Deviations from the models are likely due to the simplicity of our dynamical models, which do not allow for such known complications as dynamical substructure.

The final result of our analysis is an estimate of the activity lifetime at each spectral type. The values are given in Table 2 and shown in Figure 10. The error bars indicate the range of activity lifetimes for all of the simulations at each spectral type. The dotted line is the Hawley et al. (2000) activity-age relation. The activity lifetimes increase to later spectral types and as predicted, our results fall above the Hawley relation and extend to later spectral types. Due to the small sample size beyond a spectral type of M7, we only include lifetimes for M0-M7 dwarfs. There is a large jump in the activity lifetime at the fully convective boundary between types M3-M5, suggesting that a change in the magnetic dynamo mechanism at this boundary leads to much longer lasting magnetic activity in later type M dwarfs. The derived trend also increases our understanding of the selection effects

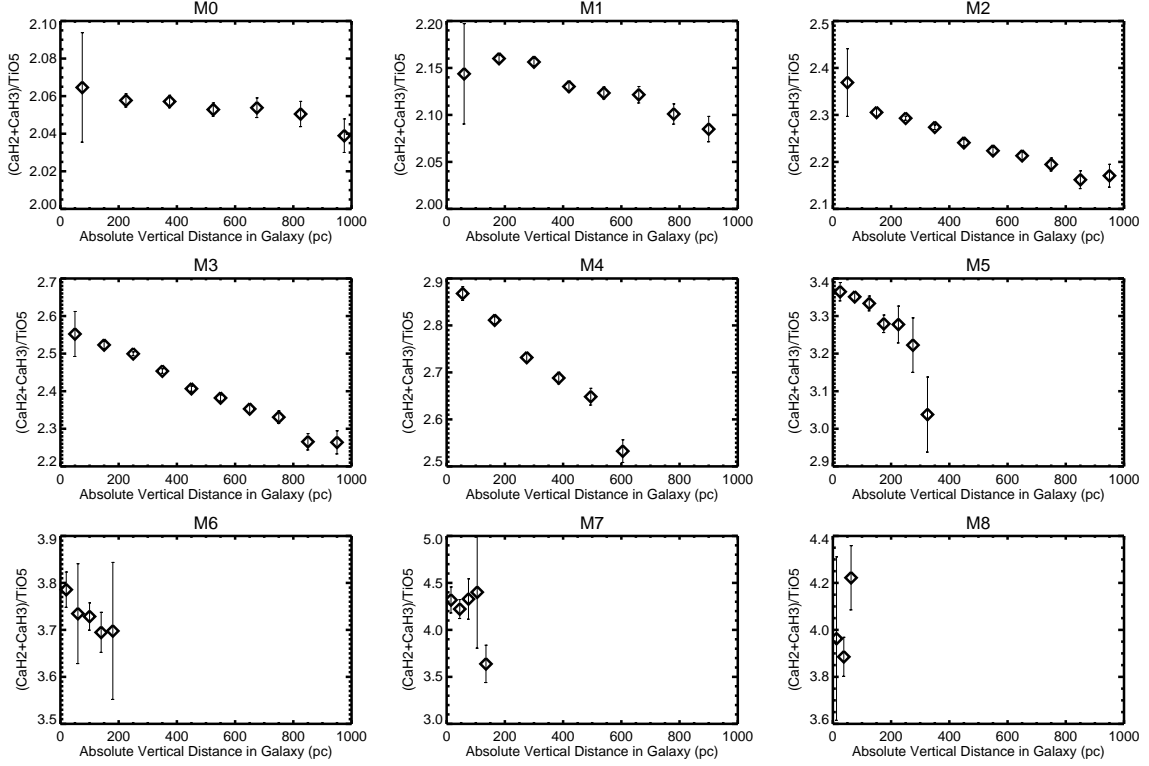


FIG. 7.— The metal sensitive ratio $(\text{CaH2}+\text{CaH3})/\text{TiO5}$ as a function of absolute vertical distance from the Plane for M0-M8 dwarfs. Stars further from the Galactic Plane are more metal-poor. Error bars represent the uncertainties in the mean values for each bin. Although we cannot yet tie this ratio to an absolute metallicity scale, our results demonstrate that future M dwarf studies should be able to determine the metallicity evolution of the Milky Way thin disk in a statistically robust way.

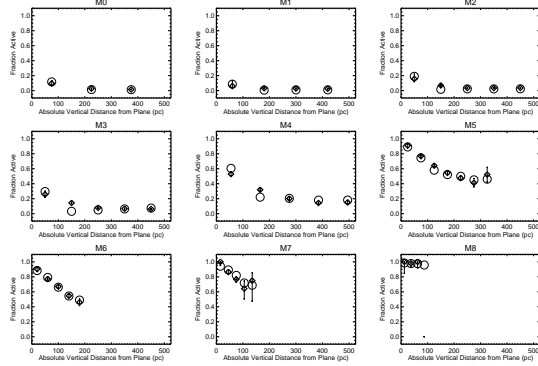


FIG. 8.— Active fraction as a function of absolute vertical distance from the Plane (diamonds) compared with the best-fit simulation data (open circles). All simulated data uses a “region of influence” of 1 pc. The simple 1-D simulations fit the observed trends well at all spectral types.

responsible for the activity fractions shown in Figures 3 and 4; later type stars are seen to be more active because they are both closer *and* their active lifetimes are longer.

5. SUMMARY

Using over 44,000 spectroscopically confirmed M and L dwarfs, we have expanded the analysis of W06 and completed a detailed study of the magnetic activity, metallicity and dynamics of cool stars in the SDSS. The results of our analysis are summarized below.

1. We have compiled the largest spectroscopic sample of low mass stars ever assembled. By matching our spectra to SDSS and 2MASS photometry, we compute the mean optical/IR colors for each spectral type with un-

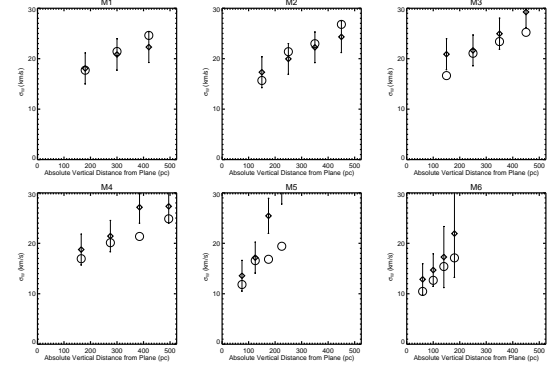


FIG. 9.— Vertical velocity dispersions as a function of vertical distance from the Plane for the DR5 sample (diamonds) compared to the simulations (open circles). Only spectral types that have large numbers of nearby (< 500 pc) stars with measured proper motions are shown. Our simple dynamical simulations are able to reproduce nearly all of the velocity data.

precedented robustness. Although these colors represent the best determination of optical/IR colors for cool stars to date, they may still be affected by the non-uniform sample selection.

2. We show that activity fractions decrease as a function of absolute height above the Galactic Plane for all M dwarf spectral types and that the magnitude and slope of this effect is different for each spectral type.

3. The amount of activity as quantified by $L_{\text{H}\alpha}/L_{\text{bol}}$ decreases slightly as a function of vertical distance from the Plane. However, $L_{\text{H}\alpha}/L_{\text{bol}}$ does not continue to decrease to the smallest detectable values, providing evidence for a rapid decrease of magnetic activity after some

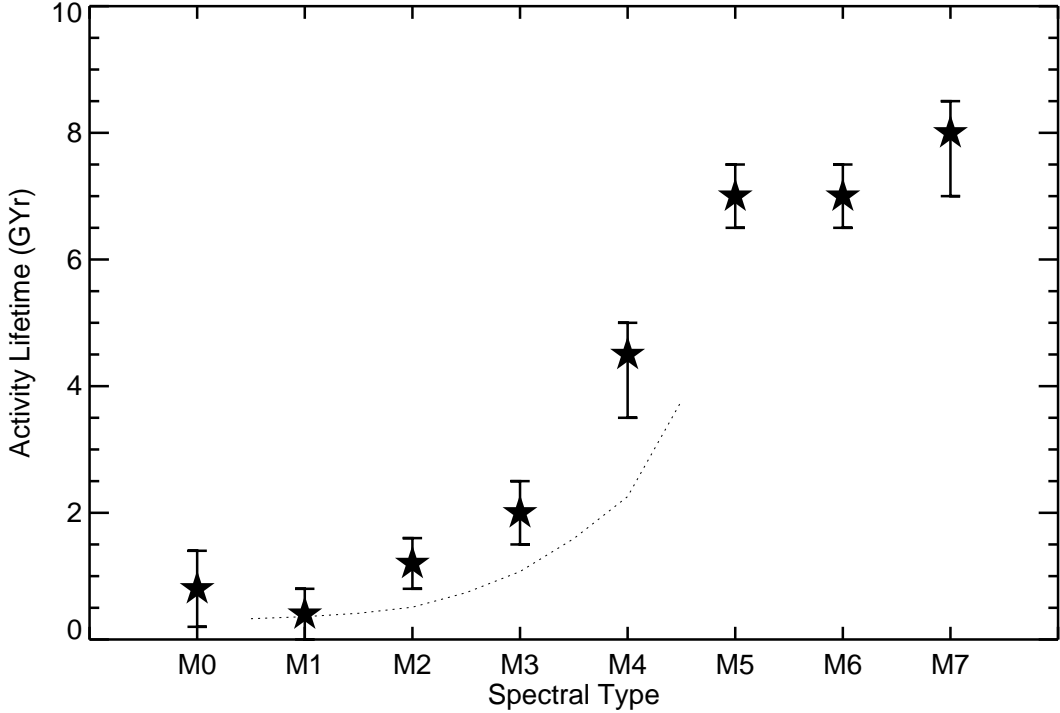


FIG. 10.— The activity lifetimes of M dwarfs as determined by comparing the DR5 spectroscopic data to the 1-D simulations (stars). The Hawley et al. (2000) age-activity relation is overplotted for comparison (dotted). As predicted, the Hawley relation provides a lower limit to the ages. We find that there is a significant increase in activity lifetimes between spectral types M3 to M5, possibly indicating a physical change in the production of magnetic fields as full convection sets in. The uncertainties indicate the spread of the model fits at each spectral type.

TABLE 2
ACTIVITY LIFETIMES
OF M DWARFS

Spectral Type	Age (Gyr)
M0	0.8 ± 0.6
M1	0.4 ± 0.4
M2	1.2 ± 0.4
M3	2.0 ± 0.5
M4	4.5 ± 1.0
M5	7.0 ± 0.5
M6	7.0 ± 0.5
M7	8.0 ± 1.0

characteristic lifetime.

4. The metallicity sensitive ratio $(\text{CaH2}+\text{CaH3})/\text{TiO5}$ also decreases with increased distance from the Plane. Although we cannot yet calibrate this ratio to an absolute metallicity scale, we suggest that future studies will be able to use data of this type to determine the metallicity evolution of the Milky Way using low mass dwarfs.

5. We use a 1-D dynamical simulation to create a realistic model of M dwarf motions and positions over the lifetime of the Galaxy and show that our models match the observed activity and velocity trends.

6. Comparing our activity data to the dynamical simulations, we derive an age-activity relation for M dwarfs for spectral types M0-M7. We find that there is a strong increase in the active lifetimes of stars in the spectral

type range from M3-M5, which may be due to the onset of full convection and subsequent change in the mechanism for producing and storing magnetic fields in the stellar interior.

This last point is the main result of the paper and deserves further elucidation. The sharp increase in activity lifetime after spectral type M3 (where the stars are predicted to become fully convective) may be an empirical indication of the change from a solar-like, rotationally-dependent magnetic dynamo in the earlier type stars, to a turbulent dynamo (that may or may not be dependent on rotation) in the later type stars. The short activity lifetimes of the early type M dwarfs would then be naturally explained by an extension of solar type rotation-activity relations (e.g. Skumanich) to these stars, and the timescale would be set by their spindown time. Although previous studies have claimed evidence for a rotation-activity relation extending past the M3 convective transition and into the brown dwarf regime (Delfosse et al. 1998; Mohanty & Basri 2003), these studies may be biased by samples of nearby, young, active M dwarfs. Future rotation studies of inactive late-type M dwarfs are needed to confirm these results.

The long activity lifetimes we have found for the fully convective stars, where the magnetic fields are presumably generated by a turbulent dynamo mechanism, set significant constraints on the operation of the dynamo and the emergence of the surface fields to power the activity. Future models must successfully predict long (several Gyr) lifetimes, and the lifetimes must be mass dependent (increasing with lower mass).

Our age-activity relation is consistent with previous findings for early type M dwarfs and we extend the relation to stars near the M dwarf/brown dwarf frontier. The faintness of M dwarfs in old star clusters limits our ability to observe this relation directly. However, future spectroscopic studies should be able to test our age-activity relation with data for clusters of known (older) ages.

Many other studies are possible with this large spectroscopic sample. Future papers will focus on the detailed dynamics of M dwarfs as probes of Galactic structure (Hawley et al. 2008; West et al. 2008), investigate the flare rate of active stars (Hilton et al. 2008) and extend our DR5 sample to the lower mass L dwarfs (Schmidt et al. 2008).

The advent of large surveys such as SDSS and 2MASS has allowed for many statistically robust studies of M dwarfs, the most numerous yet faintest stellar constituents of the Milky Way. Future large surveys such as Pan-STARRS and LSST will add much to photometric studies of low-mass stars but will not have spectroscopic components. Therefore, this SDSS low-mass star spectroscopic sample should remain useful for the foreseeable future.

6. ACKNOWLEDGMENTS

AAW acknowledges the support of NSF grant 0540567. SLH and JJB are supported by NSF grant AST02-05875 and AST067644. KRC is supported by a Spitzer Postdoctoral Fellowship. The authors would like to thank

Matthew Browning, Lucianne Walkowicz, Tom Quinn, Adam Burgasser, and Gibor Basri for useful discussions while completing this project.

Funding for the SDSS and SDSS-II has been provided by the Alfred P. Sloan Foundation, the Participating Institutions, the National Science Foundation, the U.S. Department of Energy, the National Aeronautics and Space Administration, the Japanese Monbukagakusho, the Max Planck Society, and the Higher Education Funding Council for England. The SDSS Web Site is <http://www.sdss.org/>.

The SDSS is managed by the Astrophysical Research Consortium for the Participating Institutions. The Participating Institutions are the American Museum of Natural History, Astrophysical Institute Potsdam, University of Basel, Cambridge University, Case Western Reserve University, University of Chicago, Drexel University, Fermilab, the Institute for Advanced Study, the Japan Participation Group, Johns Hopkins University, the Joint Institute for Nuclear Astrophysics, the Kavli Institute for Particle Astrophysics and Cosmology, the Korean Scientist Group, the Chinese Academy of Sciences (LAMOST), Los Alamos National Laboratory, the Max-Planck-Institute for Astronomy (MPIA), the Max-Planck-Institute for Astrophysics (MPA), New Mexico State University, Ohio State University, University of Pittsburgh, University of Portsmouth, Princeton University, the United States Naval Observatory, and the University of Washington.

REFERENCES

- Adelman-McCarthy, J. K., et al. 2007a, *ApJS*, 172, 634
 —. 2007b, *ApJS*, submitted
 Barry, D. C. 1988, *ApJ*, 334, 436
 Binney, J., Dehnen, W., & Bertelli, G. 2000, *MNRAS*, 318, 658
 Binney, J., Gerhard, O., & Spergel, D. 1997, *MNRAS*, 288, 365
 Bochanski, J. J., Munn, J. A., Hawley, S. L., West, A. A., Covey, K. R., & Schneider, D. P. 2007a, *AJ*, in press
 Bochanski, J. J., West, A. A., Hawley, S. L., & Covey, K. R. 2007b, *AJ*, 133, 531
 Bochanski, J. J., et al. 2008, *AJ*, in prep
 Burgasser, A. J., & Kirkpatrick, J. D. 2006, *ApJ*, 645, 1485
 Chabrier, G., & Baraffe, I. 1997, *A&A*, 327, 1039
 Cohen, M. 1995, *ApJ*, 444, 874
 Covey, K. R., et al. 2007, *AJ*, in press
 —. 2008, *AJ*, in prep
 Cutri, R. M., et al. 2003, 2MASS All Sky Catalog of point sources. (The IRSA 2MASS All-Sky Point Source Catalog, NASA/IPAC Infrared Science Archive. <http://irsa.ipac.caltech.edu/applications/Gator/>)
 Davenport, J. R. A., West, A. A., Matthesen, C. K., Schmieding, M., & Kobelski, A. 2006, *PASP*, 118, 1679
 Delfosse, X., Forveille, T., Perrier, C., & Mayor, M. 1998, *A&A*, 331, 581
 Eggen, O. J. 1990, *PASP*, 102, 166
 Fleming, T. A., Schmitt, J. H. M. M., & Giampapa, M. S. 1995, *ApJ*, 450, 401
 Fuchs, B., Dettbarn, C., Jahreiß, H., & Wielen, R. 2001, in *ASP Conf. Ser. 228: Dynamics of Star Clusters and the Milky Way*, ed. S. Deiters, B. Fuchs, A. Just, R. Spurzem, & R. Wielen, 235
 Fukugita, M., Ichikawa, T., Gunn, J. E., Doi, M., Shimasaku, K., & Schneider, D. P. 1996, *AJ*, 111, 1748
 Giampapa, M. S., & Liebert, J. 1986, *ApJ*, 305, 784
 Gizis, J. E. 1997, *AJ*, 113, 806
 Gizis, J. E., Monet, D. G., Reid, I. N., Kirkpatrick, J. D., Liebert, J., & Williams, R. J. 2000, *AJ*, 120, 1085
 Gizis, J. E., Reid, I. N., & Hawley, S. L. 2002, *AJ*, 123, 3356
 Gunn, J. E., et al. 1998, *AJ*, 116, 3040
 —. 2006, *AJ*, 131, 2332
 Hänninen, J., & Flynn, C. 2002, *MNRAS*, 337, 731
 Hawley, S. L., Covey, K. R., et al. 2002, *AJ*, 123, 3409
 Hawley, S. L., Gizis, J. E., & Reid, I. N. 1996, *AJ*, 112, 2799
 Hawley, S. L., Reid, I. N., & Tourtellot, J. G. 2000, in *Very Low-mass Stars and Brown Dwarfs*, Edited by R. Rebolo and M. R. Zapatero-Osorio. Published by the Cambridge University Press, UK, 2000., p.109, ed. R. Rebolo & M. R. Zapatero-Osorio, 109+
 Hawley, S. L., Tourtellot, J. G., & Reid, I. N. 1999, *AJ*, 117, 1341
 Hawley, S. L., et al. 2008, *AJ*, in prep
 Hilton, E. J., et al. 2008, *AJ*, in prep
 Hogg, D. W., Finkbeiner, D. P., Schlegel, D. J., & Gunn, J. E. 2001, *AJ*, 122, 2129
 Ivezić, Ž., et al. 2004, *Astronomische Nachrichten*, 325, 583
 Kuijken, K., & Gilmore, G. 1989, *MNRAS*, 239, 605
 Lépine, S., Shara, M. M., & Rich, R. M. 2003, *ApJ*, 585, L69
 Marshall, J. L. 2007, *AJ*, 134, 778
 Mohanty, S., & Basri, G. 2003, *ApJ*, 583, 451
 Munn, J. A., et al. 2004, *AJ*, 127, 3042
 Ng, Y. K., Bertelli, G., Chiosi, C., & Bressan, A. 1997, *A&A*, 324, 65
 Ossendrijver, M. 2003, *A&A Rev.*, 11, 287
 Parker, E. N. 1993, *ApJ*, 408, 707
 Pier, J. R., Munn, J. A., Hindsley, R. B., Hennessy, G. S., Kent, S. M., Lupton, R. H., & Ivezić, Ž. 2003, *AJ*, 125, 1559
 Press, W. H., Teukolsky, S. A., Vetterling, W. T., & Flannery, B. P. 1992, *Numerical recipes in C. The art of scientific computing* (Cambridge: University Press, —c1992, 2nd ed.)
 Rauscher, E. & Marcy, G. W. 2006, *PASP*, 118, 617
 Reid, I. N., Hawley, S. L., & Gizis, J. E. 1995, *AJ*, 110, 1838
 Reid, N., & Hawley, S. L., eds. 2005, *New light on dark stars : red dwarfs, low mass stars, brown dwarfs*, ed. N. Reid & S. L. Hawley
 Schmidt, S. J., et al. 2008, *AJ*, in prep
 Schmidt, S. J., Cruz, K. L., Bongiorno, B. J., Liebert, J. & Reid, I. N. 2007, *AJ*, 133, 2258
 Siebert, A., Bienaymé, O., & Soubiran, C. 2003, *A&A*, 399, 531
 Silvestri, N. M., et al. 2006, *AJ*, 131, 1674
 Skumanich, A. 1972, *ApJ*, 171, 565
 Smith, J. A., et al. 2002, *AJ*, 123, 2121

- Smolčić, V., et al. 2004, ApJ, 615, L141
- Soderblom, D. R., Duncan, D. K., & Johnson, D. R. H. 1991, ApJ, 375, 722
- Stauffer, J. R., Liebert, J., Giampapa, M., Macintosh, B., Reid, N., & Hamilton, D. 1994, AJ, 108, 160
- Stoughton, C., et al. 2002, AJ, 123, 485
- Strauss, M. A., et al. 2002, AJ, 124, 1810
- Thompson, M. J., Christensen-Dalsgaard, J., Miesch, M. S., & Toomre, J. 2003, ARA&A, 41, 599
- Tucker, D. L., & others. 2006, Astronomische Nachrichten, 327, 821
- Walkowicz, L. M., Hawley, S. L., & West, A. A. 2004, PASP, 116, 1105
- Weis, E. W., & Upgren, A. R. 1995, AJ, 109, 812
- West, A. A., Bochanski, J. J., Hawley, S. L., Cruz, K. L., Covey, K. R., Silvestri, N. M., Reid, I. N., & Liebert, J. 2006, AJ, 132, 2507
- West, A. A., Hawley, S. L., Walkowicz, L. M., Covey, K. R., Silvestri, N. M., Raymond, S. N., Harris, H. C., Munn, J. A., McGehee, P. M., Ivezić, Ž., & Brinkmann, J. 2004, AJ, 128, 426
- West, A. A., Walkowicz, L. M., & Hawley, S. L. 2005, PASP, 117, 706
- West, A. A., et al. 2008, AJ, in prep
- Wielen, R. 1977, A&A, 60, 263
- Wilson, O., & Woolley, R. 1970, MNRAS, 148, 463
- Woolf, V. M., & Wallerstein, G. 2006, PASP, 118, 218
- York, D. G., et al. 2000, AJ, 120, 1579